NUMERICAL COMPUTATION OF VISCOUS DRAG FOR AXISYMMETRIC UNDERWATER VEHICLES

Md. Mashud Karim[1*], Md. Mahbubar Rahman[2] and Md. Abdul Alim[3]

[1]Department of Naval Architecture and Marine Engineering, Bangladesh University of Engineering and Technology, Dhaka-1000, Bangladesh

[2]Postgraduate Student, Department of Naval Architecture and Ocean Engineering, Osaka University, Japan

[3]Dept. of Mathematics, Bangladesh University of Engineering and Technology, Dhaka-1000, Bangladesh

ABSTRACT

Simulation of flow past underwater vehicle hull form continues to grow rapidly in the field of marine hydrodynamics. With the advent of high speed computers, significant progress has been made in predicting flow characteristics around any given hull form. Although minimization of drag is one of the most important design criteria, not much effort has been given to determining viscous drag, an important parameter in the development of a new design. This paper presents finite volume method based on Reynolds-averaged Navier-Stokes (RANS) equations for computation of viscous drag. Computations are performed on bare submarine hull DREA and six axisymmetric bodies of revolution with a number of Length-Diameter (L/D) ratios ranging from 4 to 10. Shear Stress Transport (SST) k-ω model has been used to simulate turbulent flow past bodies. Finally, computed results are compared with experimental measurements and found satisfactory.

Keywords: *Axisymmetric body of revolution, underwater vehicle, viscous drag, CFD, turbulence model*

1.0   INTRODUCTION

Applications of computational fluid dynamics (CFD) to the maritime industry continue to grow as this advanced technology takes advantage of the increasing speed of computers. In the last two decades, different areas of incompressible flow modeling including grid generation techniques, solution algorithms and turbulence modeling, and computer hardware capabilities have witnessed tremendous development. In view of these developments, computational fluid dynamics (CFD) can offer a cost-effective solution to many problems in underwater vehicle hull forms. However, effective utilization of CFD for marine hydrodynamics

---

* Corresponding author: E-mail: mmkarim@name.buet.ac.bd

depends on proper selection of turbulence model, grid generation and boundary resolution.

Turbulence modeling is still a necessity as even with the emergence of high performance computing since analysis of complex flows by direct numerical simulations (DNS) is untenable. The peer approach, the large-Eddy simulation (LES), still remains expensive. Hence, simulation of underwater hydrodynamics continues to be based on the solution of the Reynolds-averaged Navier-Stokes (RANS) equations. Various researchers used turbulence modeling to simulate flow around axisymmetric bodies since late seventies. Patel and Chen [1] made an extensive review of the simulation of flow past axisymmeric bodies. Choi and Chen [2] gave calculation method for the solution of RANS equation, together with k-ε turbulence model. Sarkar et al. [3] used a low-Re k-ε model of Lam and Bremhorst [4] for simulation of flow past underwater axisymmetric bodies. In this research, SST k-ω model is used to simulate complete turbulent flow past underwater vehicle hull forms. The body used for this purpose is a standard DREA (Defence Research Establishment Atlantic) bare submarine hull [5] as shown in Figure 1 and six axisymmetric bodies of revolution based on Gertler geometry [6].
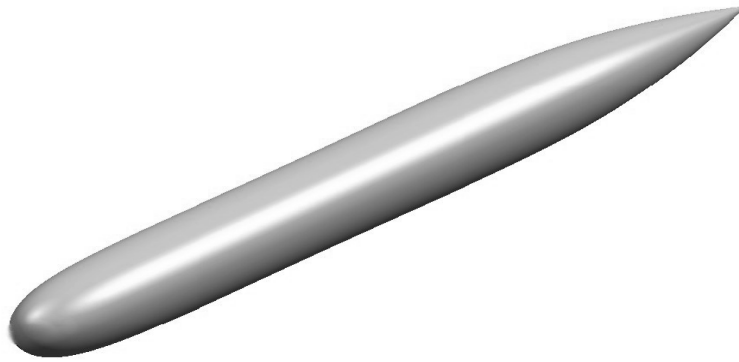
Figure 1: DREA bare submarine hull

2.0   THEORETICAL FORMULATION

For the flow past an axisymmetric underwater vehicle hull form, the continuity equation in cylindrical co-ordinate is given by:

$$\frac{\partial \rho}{\partial t} + \frac{\partial}{\partial x}(\rho v_x) + \frac{\partial}{\partial r}(\rho v_r) + \frac{\rho v_r}{r} = S_m \tag{1}$$

where x is the axial coordinate, r is the radial coordinate, v_x is the axial velocity v_r is the radial velocity and S_m is the source term (taken as zero in this study). The axial and radial momentum equations are given by:

$$\frac{\partial}{\partial t}(\rho v_x) + \frac{1}{r}\frac{\partial}{\partial x}(r\rho v_x v_x) + \frac{1}{r}\frac{\partial}{\partial r}(r\rho v_r v_x) = -\frac{\partial p}{\partial x} + F_x \qquad (2)$$

$$\frac{\partial}{\partial t}(\rho v_r) + \frac{1}{r}\frac{\partial}{\partial x}(r\rho v_x v_r) + \frac{1}{r}\frac{\partial}{\partial r}(r\rho v_r v_r) = -\frac{\partial p}{\partial r} + F_r \qquad (3)$$

where p is the static pressure and F is the external body force (taken as zero here) and

$$\nabla \cdot \vec{v} = \frac{\partial v_x}{\partial x} + \frac{\partial v_r}{\partial r} + \frac{v_r}{r}$$

2.1 The Shear-Stress Transport (SST) k-ω model

The SST k-ω turbulence model is a two-equation eddy-viscosity model developed by Menter [7] to effectively blend the robust and accurate formulation of the k-ω model in the near-wall region with the free-stream independence of the k-e model in the far field. To achieve this, the k-e model is converted into a k-ω formulation. The SST k-ω model is similar to the standard k-ω model, but includes the following refinements:

- The standard k-ω model and the transformed k-e model are both multiplied by a blending function and both models are added together.
- The blending function is designed to be one in the near-wall region, which activates the standard k-ω model, and zero away from the surface, which activates the transformed k-e model.
- The SST model incorporates a damped cross-diffusion derivative term in the ω equation.
- The definition of the turbulent viscosity is modified to account for the transport of the turbulent shear stress.
- The modeling constants are different.

These features make the SST k-ω model more accurate and reliable for a wider class of flows (e.g., adverse pressure gradient flows, airfoils, transonic shock waves) than the standard k-ω model. The shear-stress transport (SST) k-ω model is so named because the definition of the turbulent viscosity is modified to account for the transport of the principal turbulent shear stress. The use of a k-ω formulation in the inner parts of the boundary layer [8] makes the model directly usable all the way down to the wall through the visous sub-layer, hence the SST k-ω model can be used as a Low-Re turbulence model without any extra damping functions. The SST formulation also switches to a k-ε behaviour in the free-stream and thereby avoids the common k-ω problem that the model is too sensitive to the inlet free-stream turbulence properties. It is this feature that gives the SST k-ω model an advantage in terms of performance over both the standard k-ω model and the standard k-ε model. Other modifications include the addition of a cross-diffusion term in the ω equation and a blending function to ensure that the model equations behave appropriately in both the near-wall and far-field zones.

Transport equations for the SST k-ω model are given by:

$$\frac{\partial}{\partial t}(\rho k) + \frac{\partial}{\partial x_i}(\rho k u_i) = \frac{\partial}{\partial x_j}\left(\Gamma_k \frac{\partial k}{\partial x_j}\right) + \widetilde{G}_k - Y_k + S_k \tag{4}$$

$$\frac{\partial}{\partial t}(\rho \omega) + \frac{\partial}{\partial x_i}(\rho \omega u_i) = \frac{\partial}{\partial x_j}\left(\Gamma_\omega \frac{\partial \omega}{\partial x_j}\right) + G_\omega - Y_\omega + D_\omega + S_\omega \tag{5}$$

In these equations, $\widetilde{G}_k$ represents the generation of turbulence kinetic energy due to mean velocity gradients, G_ω represents the generation of ω, Γ_k and Γ_ω represent the effective diffusivity of k and ω, respectively, Y_k and Y_ω represent the dissipation of k and ω due to turbulence, D_ω represents the cross-diffusion term, S_k and S_ω are user-defined source terms.

2.2 Boundary Conditions
Since the geometry of an axisymmetric underwater hull is, in effect, a half body section rotated about an axis parallel to the free stream velocity, the bottom boundary of the domain is modeled as an axis boundary. Additionally, the left and top boundaries of the domain are modeled as velocity inlet, the right boundary is modeled as an outflow boundary, and the surface of the body itself is modeled as a wall.

2.3 Viscous Drag
The viscous drag of a body is generally derivable from the boundary-layer flow either on the basis of the local forces acting on the surface of the body or on the basis of the velocity profile of the wake far downstream. The local hydrodynamic force on a unit of surface area is resolvable into a surface shearing stress or local skin friction tangent to the body surface and a pressure p normal to the surface. The summation over the whole body surface of the axial components of the local skin friction and of the pressure gives, respectively, the skin-friction drag D_f and the pressure drag D_p which for a body of revolution in axisymmetric flow become

$$D_f = 2\pi \int_0^{x_e} r_w \tau_w \cos \alpha \, dx \tag{6}$$

$$D_p = 2\pi \int_0^{x_e} r_w p \sin \alpha \, dx \tag{7}$$

where, r_w is the radius from the axis to the body surface, α is the arc length along the meridian profile, and x_e is the total arc length of the body from nose to tail.

The sum of the two drags then constitutes the total viscous drag, D or $D = D_f + D_p$ The drag coefficient C_D and the pressure coefficient, C_p based on some appropriate reference area A are given by:

$$C_D = \frac{D}{0.5\,\rho U_\infty^2 A} \quad \text{and} \quad C_p = \frac{p - p_\infty}{0.5\,\rho U_\infty^2 A} \tag{8}$$

where p_∞ is pressure of free stream and U_∞ is free stream velocity.

3.0 METHODOLOGY

3.1 Computational Method and Domain
The axisymmetric problem with appropriate boundary conditions is solved over a finite computational domain. The computational domain extended 1.0L upstream of the leading edge of the axisymmetric body, 1.0L above the body surface and 2.0L downstream from the trailing edge; where L is the overall length of the body. The solution domain is found large enough to capture the entire viscous-inviscid interaction and the wake development.

A finite volume method [9, 10] is employed to obtain a solution of the Reynolds averaged Navier-Stokes equations. The coupling between the pressure and velocity fields is achieved using PISO algorithm [9]. A second order upwind scheme is used for the convection and the central-differencing scheme for diffusion terms.

3.2 Geometry of Axisymmetric Underwater Vehicle (AUV) Hull Form
Axisymmetric bodies are ideal candidates for a parametric study with their easily defined geometry, straightforward grid generation, and available experimental data. At first the bare submarine hull DREA and then a systematic series of mathematically defined bodies of revolution is studied.

3.3 Geometry of Bare Submarine Hull DREA
The parent axisymmetric hull form with maximum length, l and diameter, d can be divided into three regions, i.e., nose, mid body and tail.

(i) The nose can be represented by:

$$\frac{r_1(x)}{l} = \frac{d}{l}\left[2.56905\sqrt{\frac{x}{l}} - 3.48055\frac{x}{l} + 0.49848\left(\frac{x}{l}\right)^2 + 3.40732\left(\frac{x}{l}\right)^3\right] \quad ;0 \le \frac{x}{l} \le 0.2$$

(ii) The mid body (circular cylinder) is given by:

$$\frac{r_2(x)}{l} = \frac{d}{2l} \quad ;0.2 \le \frac{x}{l} \le 1 - \frac{3d}{l}$$

(iii) The tail is represented by:

$$\frac{r_3(x)}{l} = \frac{d}{2l} - \frac{l}{18d}\left[\frac{x}{l} - \left(1 - \frac{3d}{l}\right)\right]^2 \quad ;1 - \frac{3d}{l} \le \frac{x}{l} \le 1$$

13
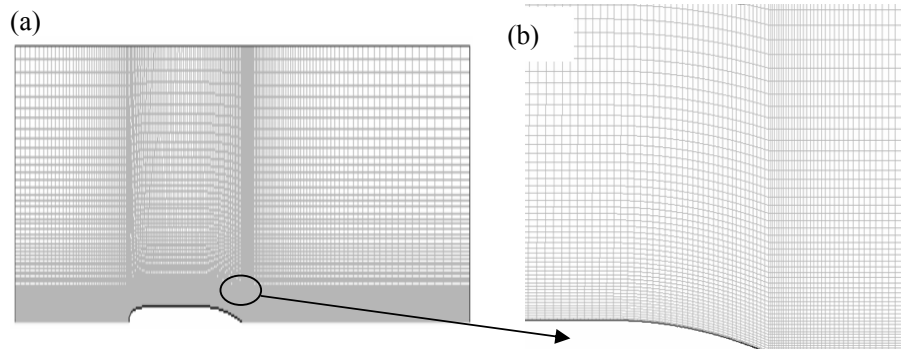
Figure 2: (a) Grid of flow domain around DREA bare submarine hull
(b) Enlarged view of grid near stern side

3.4 Geometry of Axisymmetric Body of Revolution

Each body is defined by a sixth-degree polynomial [6]. Six axisymmetric bodies were generated with length-to-diameter ratios (*L/D*) ranging from four to ten.

3.5 Grid Generation

A body-fitted H-type grid is used. In external flow simulations using SST *k-ω* the computational grid should be in such a way that sufficient number of grid points lie within the laminar sublayer of the ensuing boundary layer. In order to ensure this, usually the y^+ criterion is used. y^+ is a non-dimensional distance from the body wall and is defined as $y^+ = yu_\tau/\nu$, where $u_{\tau=} \tau_\omega/\rho$ is friction velocity and ν kinematic viscosity. The y^+ criterion states that first grid point normal to the body wall should not lie beyond $y^+ = 4.0$ and for reasonable accuracy at least five points should lie with in $y^+ = 11.5$ [4]. A typical grid layout around bare submarine hull is shown in Figure 2.

4.0 RESULTS AND DISCUSSION

The computation of drag coefficient for bare submarine hull DREA is performed at Reynolds number of 2.3 x 10^7 and shown in Table 1. From the table, it is seen that the computed value agrees well with the experimental result [5]. Table 2 shows the comparison of predicted and experimental drag coefficients [12, 13] for different *L/D* ratios of axisymmetric body of revolution at Reynolds No. of 2.0x10^7. There exists a close agreement between them.

Table 1: Comparison of computed drag coefficients with experimental
values for submarine hull DREA

	C_D (Present)	C_D (Exp.)	C_D (Baker, 2004)
Submarine hull DREA	0.00104	0.00123 ±0.000314	0.00167

Table 2: Comparison of computed drag coefficients with experimental
values for different *L/D* ratios of AUV

L/D	$C_D (\times10^{-3})$ (Present)	$C_D (\times10^{-3})$ (Exp)
4	3.435	3.208
5	3.140	2.988
6	3.020	2.848
8	2.958	2.718
9	2.893	-
10	2.822	2.703

Drag convergence history is shown in Figure 3. Contours of pressure around bare submarine hull DREA is shown in Figure 4. Figure 5 shows the plot of velocity vectors around the hull. The pressure coefficient, C_p around the hull is shown in Figure 6. At first, the value of pressure coefficient decreases near the leading edge after which it increases and becomes constant around the parallel middle body. Near after body the curve dips for a while and then moves up. The curve of wall shear stress as shown in Figure 7 has opposite tendency. The curve of radial shear stress as shown in Figure 8 has convex shape at the after body of the hull. The nature of the curve of skin friction coefficient as shown in Figure 9 follows similar trend of the curve of wall shear stress which is usual.

Contour of pressure, velocity vectors, variations of pressure coefficient, wall shear stress, radial wall shear stress and skin friction of AUV having *L/D* ratio of 6 are shown in Figures 10-15. Trends of curves are almost similar to those of submarine hull except little changes near nose and tail due to different shapes. From enlarged view of velocity vectors, velocity changes within the boundary layer and vortex near stern are clearly visible as shown in Figure 11.
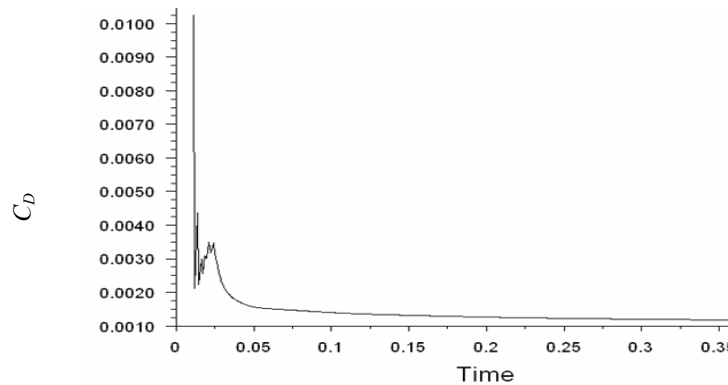
Figure 3: Drag convergence history

Figure 4: Contours of pressure around bare submarine hull DREA (filled)
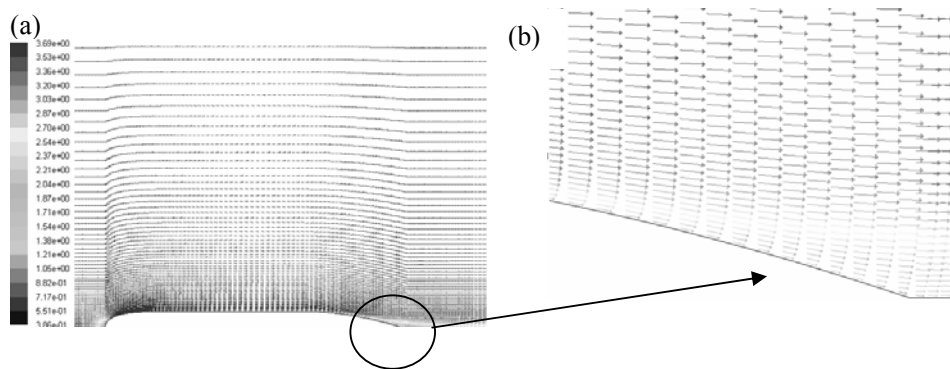
Figure 5: (a) Plot of velocity vectors around DREA (b) enlarged view of velocity vectors near stern
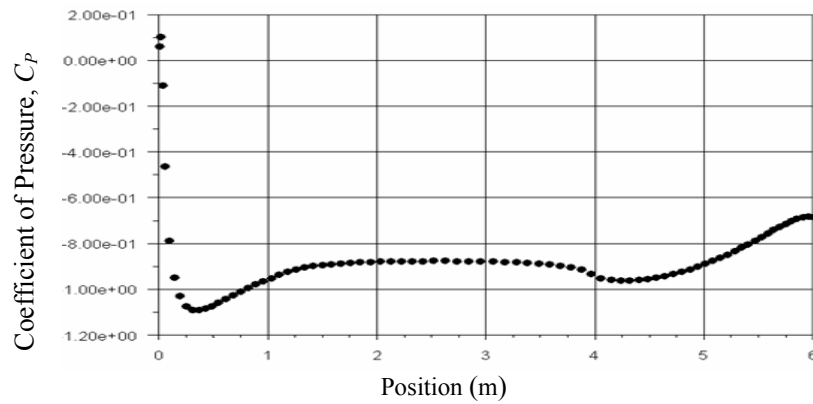
Figure 6: Variation of pressure coefficient, C_p around bare submarine hull DREA
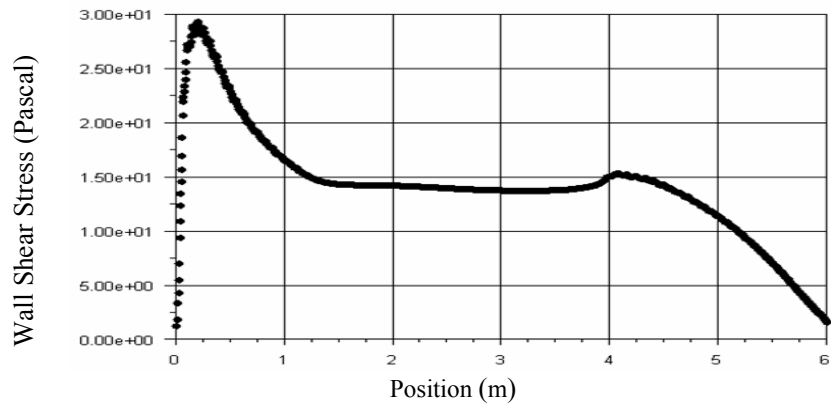
Figure 7: Variation of skin friction coefficient on the surface of DREA
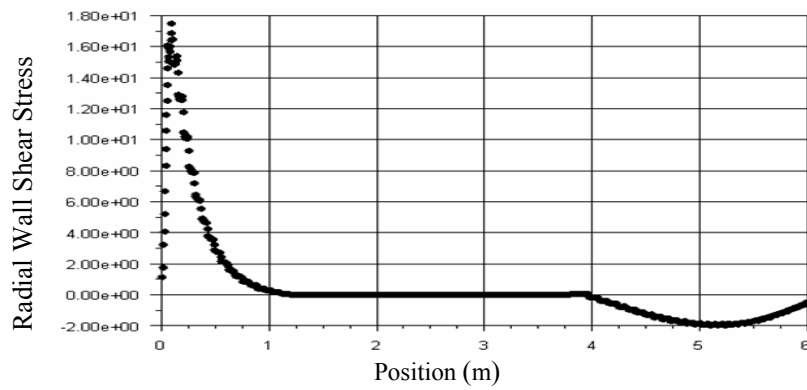
Figure 8: Variation of radial wall shear stress for DREA
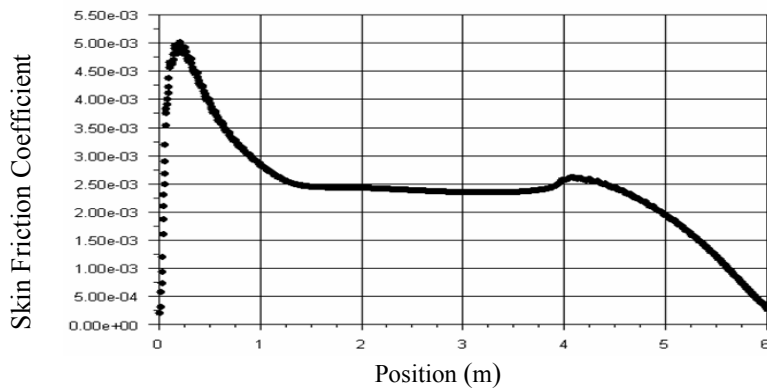
Figure 9: Variation of skin friction coefficient on the surface of DREA

Figure 10: Contour of pressure around the surface of AUV (*L/D*=6)
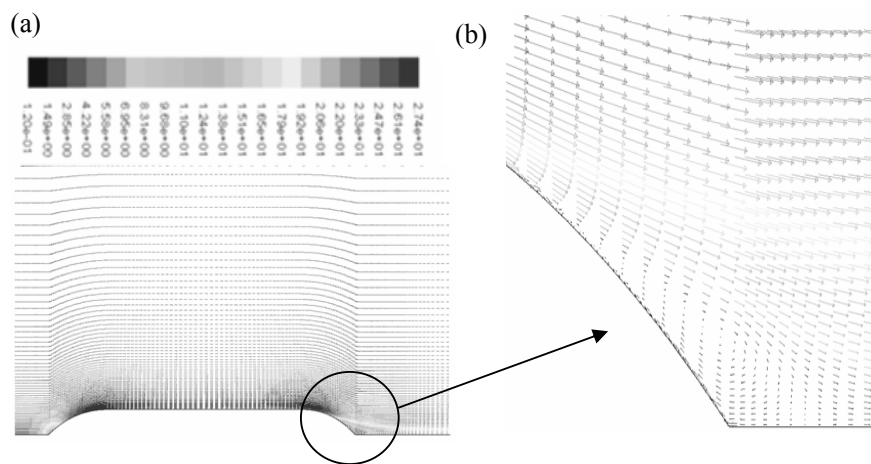
Figure 11: (a) Plot of velocity vector (b) Enlarged view of velocity vector near body
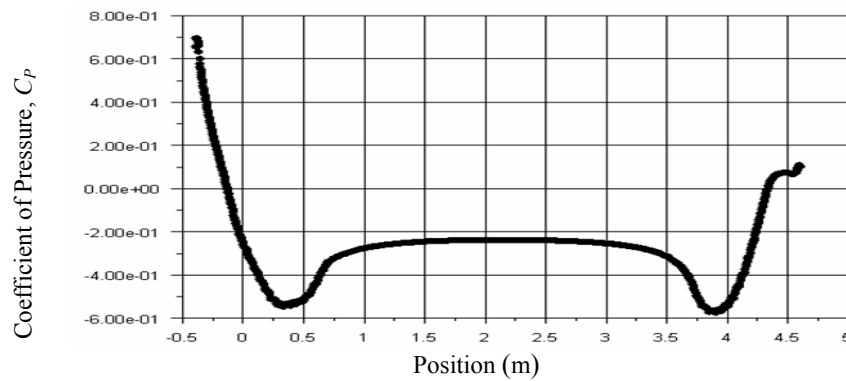
Figure 12: Variation of pressure coefficient around AUV (*L/D* = 6)
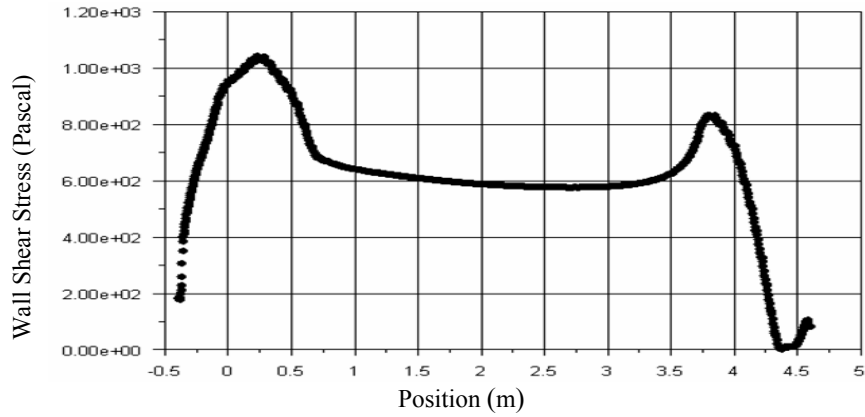
Figure 13: Variation of wall shear stress on AUV (*L/D* =6)
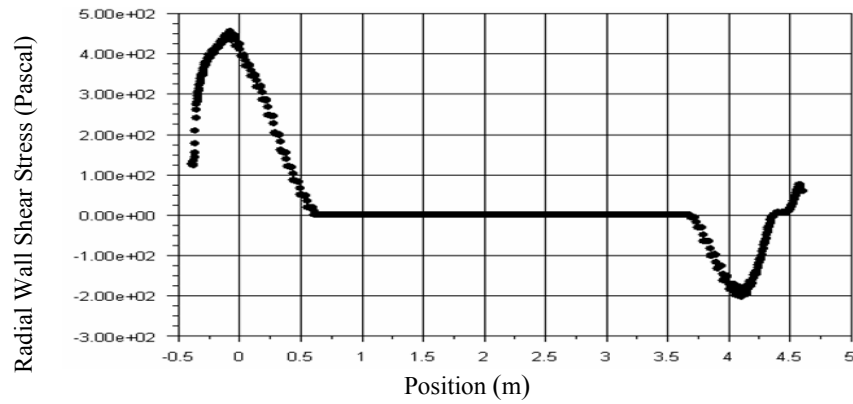
Figure 14: Variation of radial wall shear stress on AUV (*L/D* =6)
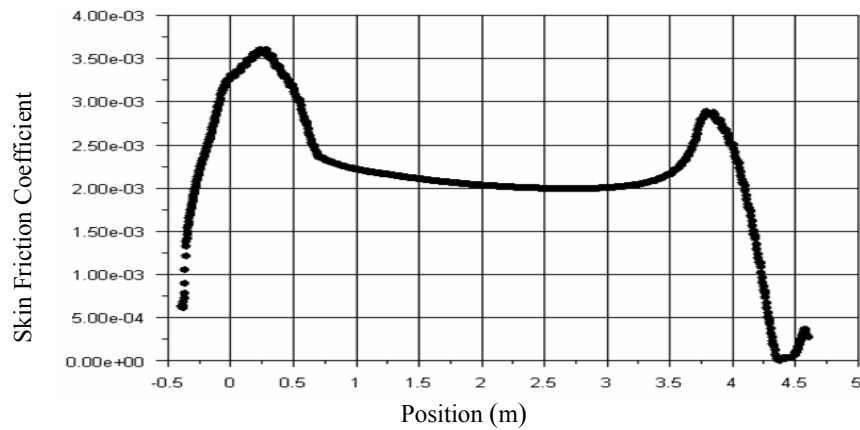
Figure 15: Variation of skin friction coefficient on AUV (*L/D* =6)

The curve of pressure coefficient is almost symmetric about the midpoint of AUV except at two ends. Each of the curves of wall shear stress (shown in Figure 13) and skin friction coefficient (shown in Figure 15) have a saddle shape at the middle portion of the body.

5.0   CONCLUSIONS

Numerical computation of viscous drag for axisymmetric underwater vehicle is performed in this research using finite volume method based on Reynolds averaged Navier-Stokes equations. Shear Stress Transport (SST) k-ω model has been used to simulate fully turbulent flow past axisymmetric underwater body. The computed results show well agreement with experimental measurements.

NOMENCLATURE

A	reference area
C_D	drag coefficient
C_p	pressure coefficient
D	diameter of the body
D_f	skin-friction drag
D_p	pressure drag
D_ω	cross-diffusion term
F	external body forces
$\tilde{G}_k$	generation of turbulence kinetic energy due to mean velocity gradients
G_ω	generation of ω
K	kinetic energy
L	length of the body
p	static pressure
p_∞	pressure of free stream
r	radial coordinate
Re	Reynolds number
r_w	radius from the axis to the body surface
S_m	source term
S_k, S_ω	user-defined source terms
t	time
u_τ	friction velocity
U_∞	free stream velocity
v_x, v_r	axial and radial velocity
x	axial and radial coordinate
x_e	arc length of the body from nose to tail
Y_k, Y_ω	dissipation of k and ω due to turbulence
y^+	non-dimensional distance from the body wall
α	arc length along the meridian profile
ε	dissipation
ω	specific dissipation
ν	kinematic viscosity

Γ_k effective diffusivity of *k*
Γ_ω effective diffusivity of ω

REFERENCES

1. Patel, V.C. and Chen, H.C., 1986. Flow over tail and in wake of axisymmetric bodies: review of the state of the art, *Journal of Ship Research*, Vol. 30, No. 3, 202-314.
2. Choi, S.K. and Chen, C.J., 1990. Laminar and turbulent flows past two dimensional and axisymmetric bodies, *Iowa Institute of Hydraulic Research, IIHR Report 334-II*.
3. Sarkar, T., Sayer, P.G. and Fraser, S.M., 1997. A study of autonomous underwater vehicle hull forms using computational fluid dynamics, *International Journal for Numerical Methods in Fluids*, Vol. 25, 1301-1313.
4. Lam, C.K.G. and Bremhorst, K., 1981. A modified form of the k-e model for predicting wall turbulence, *ASME Journal Fluid Engineering*, Vol.103, 456.
5. Baker, C., 2004. Estimating drag forces on submarine hulls, *Report DRDC Atlantic* CR 2004-125, Defence R&D Canada – Atlantic.
6. Gertler, M., 1950. Resistance experiments on a systematic series of streamlined bodies of revolution for application to the design of high speed submarines, *DTMB Report* C-297.
7. Menter, F.R., 1994. Two-equation eddy-viscosity turbulence models for engineering applications, *AIAA Journal*, 32(8):1598-1605.
8. Schlichting, H., 1966. *Boundary Layer Theory*, McGraw-Hill, New York.
9. Versteeg, H.K. and Malalasekera, W., 1995. *An Introduction to Computational Fluid Dynamics the Finite Volume Method*, Longman Scientific and Technical, U.K.
10. Cebeci, T., Shao, J.R., Kafyeke, F. and Laurendeau, E., 2005. *Computational Fluid Dynamics for Engineers*, Horizons Publishing Inc., Long Beach, California.
11. Baldwin, B.S. and Lomax, H., 1978. Thin layer approximation and algebraic model for separated turbulent flows, *AIAA 16th Aerospace Sciences Meeting*.
12. White, N.M., 1977. A comparison between a simple drag formula and experimental drag data for bodies of revolution, *DTNSRDC Report 77-0028*.
13. White, N.M., 1978. A comparison between the drags predicted by boundary layer theory and experimental drag data for bodies of revolution, *DTNSRDC SPD-784-01*.